JOURNAL OF INTERNATIONAL CRISIS AND RISK COMMUNICATION RESEARCH
ISSN: 2576-0017
2024, VOL 7, NO S8

How to diagnose common lung diseases using chest imaging

Rahmah Yousef Alshaqaqiq[1], Bandar Farhan Alruwaili[2], Ali Hussain Alabbad[3], Nasreen Ahmad Albagshi[4], Samiah Ahmed Alturki[5], Zahra Radhi Alibrahim[6], Abdulaziz Ahmad Alturki[7], SherifahkhalidAlzamil[8], Mohammed Abdulaziz Alsultan[9], Thamer Farhan Alruwaili[10], Ashraf Abdulmohsen Salman Al Kuwaiti[11], Noha Ahmed Abdulrahman Al-Odail[12], Ali Hussain Hussain Alnuwaysir[13], Rawan Ameer Almarzouq[14], Abdulrahman Abdulghani Alrashed[15].

1. Medical specialist, King Fahad hospital in alhsa, Ministry of Health, Kingdom of Saudi Arabia. RAlshaqaqiq@moh.gov.sa
2. Respiratory Therapist, pmmc SAKAKA Aljouf, Ministry of Health, Kingdom of Saudi Arabia. Bamderr606@gmail.com
3. Respiratory therapist, Prince muteb bin abdulaziz (PMH), Skaka, Ministry of Health, Kingdom of Saudi Arabia. Alihuss20177@gmail.com
4. x-ray technician, Ministry of Health Branch in Al-Ahssa, Ministry of Health, Kingdom of Saudi Arabia. Nalbagshi@moh.gov.sa
5. Nurse technician, Ministry Of Health Branch in Al-Ahssa, Ministry of Health, Kingdom of Saudi Arabia. Saaalturki@moh.gov.sa
6. Radiological Technology (specialist), Ministry of Health Branch in Al-Ahssa, Ministry of Health, Kingdom of Saudi Arabia. zralibrahim@moh.gov.sa
7. Nurse technician, King fahad hospital in hufof, Ministry of Health, Kingdom of Saudi Arabia. Abahalturki@moh.gov.sa
8. Nursing specialist, Ministry of health branch in Al-Ahssa, Ministry of Health, Kingdom of Saudi Arabia. Skalzamil@moh.gov.sa
9. Psychiatrist, Al Hasa Mental hospital, Ministry of Health, Kingdom of Saudi Arabia. Dr.msultan@hotmail.com
10. Radiology specialist, General Suwair Hospital, Ministry of Health, Kingdom of Saudi Arabia. T101010f@gmail.com
11. Nursing, KFHH, Ministry of Health, Kingdom of Saudi Arabia. aalkuwaiti@moh.gov.sa
12. Nursing Technician, Mental health hospital hufof, Ministry of Health, Kingdom of Saudi Arabia. nalodail@moh.gov.sa
13. X-ray tech, King faisal general hospital alhassa, Ministry of Health, Kingdom of Saudi Arabia. ahalnuwaysir@moh.sa
14. Respiratory therapist, domataljandal general hospital aljouf, Ministry of Health, Kingdom of Saudi Arabia. ralmarzouq@moh.gov.sa
15. Respiratory therapy, King abdulaziz hospital cardiac center, Ministry of Health, Kingdom of Saudi Arabia. D7miiii1994@gmail.com

Abstract

Chest CT imaging plays a crucial role in diagnosing various pulmonary diseases. Despite the diverse clinical presentations, imaging patterns can be categorized into distinct groups, often identified using metaphoric radiological signs. Some signs are pathognomonic for specific diseases, while others narrow the differential diagnosis. Recognizing these imaging patterns and their diagnostic implications is essential for pulmonologists. This pictorial review presents significant chest CT scan signs and their associated pulmonary diseases, emphasizing their description in the context of increasing reliance on CT imaging. Visual memory and iconographic learning have become integral to radiological language, linking CT findings with naturalistic images or symbolic representations to enhance concept assimilation and retention. Familiarity with these signs also improves diagnostic specificity due to the strong correlation between imaging features and particular thoracic diseases. The review covers various signs, including the air bronchogram, air crescent, arcade-like, atoll, cheerios, crazy paving, comet tail, dark bronchus, doughnut, eggshell calcifications, feeding vessel, finger-in-glove, Fleischner, galaxy, ginkgo leaf, Golden S, halo, headcheese, honeycombing, interface, Monod, mosaic attenuation, Oreo cookie, polo mint, popcorn calcification, positive bronchus, railway track, scimitar, signet ring, snowstorm, sunburst, tree-in-bud, and tram track signs. The review also briefly discusses miscellaneous signs like the serpent, water lily, cervicothoracic, hilum overlay, deep sulcus, Hampton's hump, and Swiss cheese signs. Understanding these radiological signs strengthens diagnostic accuracy and contributes to improved patient outcomes in pulmonary medicine.

Keywords: lung diseases, chest imaging, CT

Introduction

Chest CT imaging serves a pivotal role in diagnosing a range of pulmonary diseases. Despite the variation in clinical presentations of pulmonary diseases, the associated imaging patterns can generally be

categorized into a limited number of distinct groups. Metaphoric radiological signs have been extensively utilized to identify and simplify the interpretation of these patterns. Some of these signs, well-documented in radiological literature, are pathognomonic for specific diseases, while others assist in narrowing the differential diagnosis. These signs create a unique association between imaging patterns and the underlying disease processes.

Recognizing these imaging patterns and understanding their diagnostic implications is essential for pulmonologists. This review presents a pictorial essay of significant chest CT scan signs and the pulmonary diseases they indicate. While some of these signs are identifiable in both chest radiographs and CT imaging, this review emphasizes their description in the context of the increasing reliance on CT imaging as an initial diagnostic modality. The Fleischner Society, in 2008, categorized imaging terms used to describe key thoracic radiological signs, updating prior glossaries from 1984 and 1996 (Hansell et al., 2008). The glossary includes illustrative radiological examples of these terms, providing a valuable reference for radiologists. Several terms, such as the "atoll sign" or "crazy paving sign," draw from symbols or naturalistic images, offering an intuitive and expedited understanding of the associated radiological patterns.

Human cognition employs diverse learning mechanisms, tailored to individual ways of sensing, processing, and recalling information. The association of radiological findings with symbols and images serves as an effective strategy to enhance concept assimilation and retention. Visual memory and iconographic learning have thus become integral to radiological language, often linking CT and X-ray findings with naturalistic images or symbolic representations. This approach facilitates the creation of subconscious emotional connections to images, strengthening memory and simplifying complex learning processes. Furthermore, familiarity with these radiological signs enhances diagnostic specificity due to the strong correlation between imaging features and particular thoracic diseases.

The primary aim of this pictorial review is to present an iconographic interpretation of the glossary terms associated with thoracic radiological findings. Each finding is described alongside its symbolic, naturalistic, and schematic representations to provide a comprehensive understanding.

Air Bronchogram

As defined in the Fleischner Society glossary, the air bronchogram sign refers to the visualization of air-filled bronchial structures, which appear strongly hypodense on CT images within areas of consolidation in the surrounding pulmonary parenchyma (Fig. 1). Recognized as a cornerstone of pulmonary radiological diagnosis, this sign was first documentedby Remy J. It is observed in numerous pathological processes that fill alveolar air spaces, such as pneumonia, edema, infarction, pulmonary hemorrhage, aspiration, or trauma. These conditions may manifest the air bronchogram sign on both chest radiographs and CT scans.

Pulmonary edema, associated with cardiac dysfunction and fluid accumulation at the interstitial and alveolar levels, frequently exhibits the air bronchogram sign. In cases of edema resulting from acute respiratory distress syndrome (ARDS), this sign appears without cardiomegaly, and the consolidations show a patchy, peripheral distribution. Non-obstructive pulmonary atelectasis often presents with the air bronchogram sign in the lower lobes, usually accompanied by reduced lung volume. Persistent infectious consolidations displaying the air bronchogram sign, even after extended antibiotic therapy, may raise suspicion for pulmonary adenocarcinoma with a lepidic growth pattern or pulmonary lymphoma (Algın et al., 2011; Khan et al., 2009).

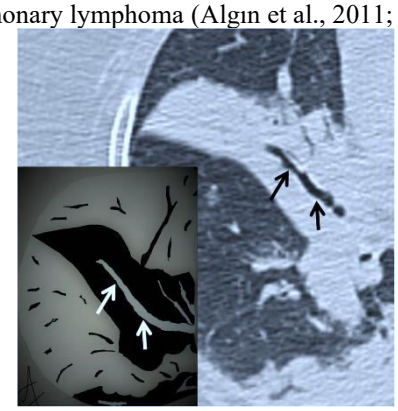

fig. 1

Air Crescent Sign

The air crescent sign, better appreciated on multidetector computed tomography (MDCT), is characterized by the presence of air surrounding invasive or semi-invasive aspergillosis lesions (Fig. 2). While this sign is not exclusive to infectious aspergillosis, its description dates to 1975 when Bard and Hassani identified the "crescent sign" in pulmonary hematomas, noting its non-specificity for "coin-lesions". In 1979, Curtis et al. documented the air crescent sign in invasive aspergillosis cases.

Aspergillus, a pathogenic microorganism, proliferates in the bronchial airways and subsequently invades the bloodstream via bronchial arteries, leading to thrombosis. This vascular obliteration causes necrosis and cavitation within the lesions. In invasive aspergillosis, MDCT images typically reveal areas of increased density with peripheral ground-glass opacities or thickening, as well as multiple irregular peribronchial nodules. Approximately two weeks after these lesions appear, necrosis and cavitation ensue, culminating in the formation of the air crescent sign within 20 days. This sign is attributed to the peripheral resorption of necrotic tissue in the lesion's central portion, with the residual area being replaced by air.

The air crescent sign is present in roughly 50% of patients with invasive aspergillosis. The resorption of necrotic tissue coincides with an improved prognosis and progressive recovery from the infection (Yella et al., 2005).

Several authors have reported that the air crescent sign may also be identified in necrotic regions of the pulmonary parenchyma resulting from various causes, including tuberculosis, abscesses, carcinomas, or parasitic lesions such as hydatidosis.

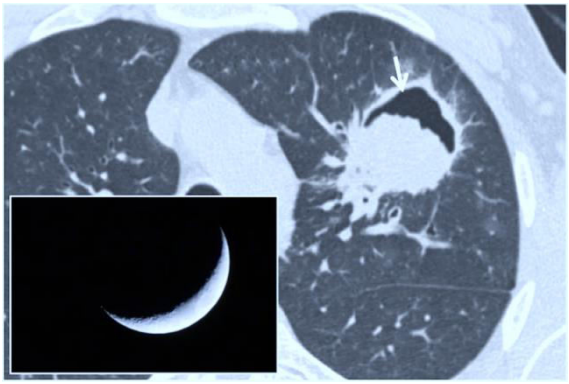

fig. 2

Arcade-Like Sign

The arcade-like sign is a characteristic radiological feature associated with perilobular fibrosis, commonly observed in cryptogenic organizing pneumonia (COP). Ujita et al. identified perilobular fibrosis exhibiting an “arch” pattern in more than half of the cases of COP. This sign may also correspond to perilobular inflammation. Radiologically, it presents as curved or arched consolidation bands with indistinct margins, distributed around the secondary pulmonary lobules (Fig. 3). Frequently, these bands extend to the pleural surface.

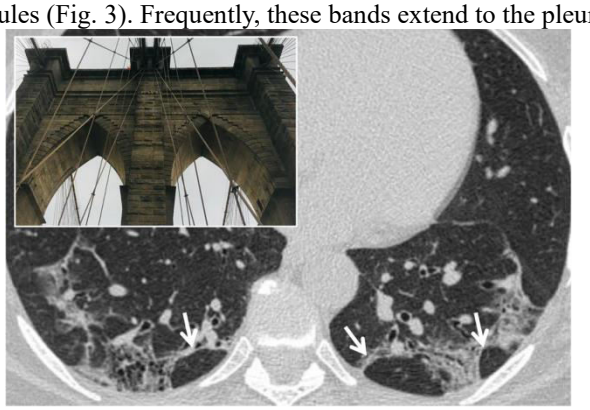

fig. 3

Atoll Sign

The atoll sign, also referred to as the "reversed halo sign," is characterized by an area of central ground-glass opacity surrounded by a ring of denser parenchymal consolidation extending for at least three-quarters of the circumference and with a thickness of at least 2 mm (Fig. 4). First described by Zompatori et al. the term "atoll" was used in a case report describing ring-shaped opacities associated with bronchiolitis obliterans organizing pneumonia (BOOP). The sign's pathogenesis involves inflammation of the alveolar septa and the accumulation of cellular debris within the alveoli, leading to the central ground-glass opacity and the peripheral granulation tissue thickening. Initially deemed highly specific to COP and BOOP, this radiological feature was described by Voloudaki et al. as "crescentic and ring-shaped opacities".

Subsequently, the atoll sign has been associated with a broad spectrum of pulmonary diseases (Marchiori et al., 2011), including atypical sarcoidosis, granulomatosis with polyangiitis, Pneumocystis jirovecii pneumonia, adenocarcinomas, pulmonary infarctions, or post-radiation therapy changes (notably in the first 4–12 weeks after treatment) (Godoy et al., 2012). Marchiori et al. further described the presence of the atoll sign in both infectious and non-infectious pulmonary diseases. Among infectious conditions, it has been observed in cases of paracoccidioidomycosis or zygomycosis. This sign is also noted in invasive fungal infections, particularly in immunocompromised individuals with conditions such as leukemia or graft-versus-host disease.

In 2014, Legouge et al. documented a case of pulmonary mucormycosis in a neutropenic leukemic patient exhibiting the reversed halo sign (Legouge et al., 2014).

Additionally, the atoll sign—when accompanied by centrilobular nodules—may signify active pulmonary tuberculosis. In granulomatous diseases, the ring structure of the reverse halo sign may exhibit nodular characteristics. Non-infectious conditions, such as COP, Wegener granulomatosis, lymphomatoid granulomatosis, and sarcoidosis, may also display this sign. Due to its occurrence across a wide array of pulmonary conditions, the atoll sign is considered a non-specific radiological feature.

Recently, Marchiori et al. described two imaging patterns associated with the reverse halo sign: nodular and reticular (Marchiori et al., 2015). The nodular pattern features nodules at the border or within the reverse halo sign and is linked to granulomatous disorders, such as tuberculosis and sarcoidosis. Conversely, the reticular pattern, characterized by reticulations within the reverse halo sign, is associated with invasive fungal infections in immunocompromised patients or pulmonary infarctions in immunocompetent individuals.

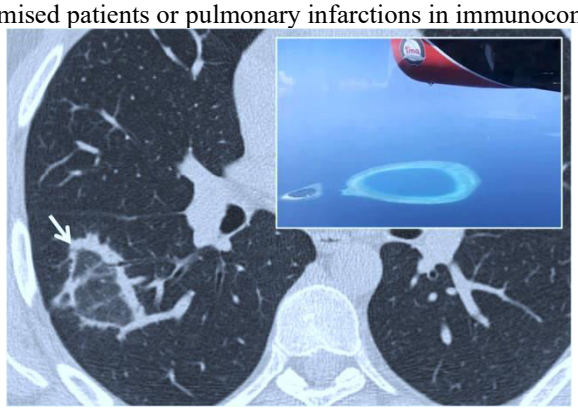

fig. 4

Cheerios Sign

The cheerios sign is a radiological finding seen in axial CT images. It consists of pulmonary nodules featuring a small central air cavity connected to a patent bronchus (Fig. 5). This sign results from cellular proliferation, either malignant or benign, around an unobstructed bronchial branch. Initially described by Reed and O'Neil this sign was associated with the development of low-grade pulmonary adenocarcinomas. Histologically, tumors reproducing the cheerios sign include adenocarcinoma in situ, minimally invasive adenocarcinoma, invasive adenocarcinoma with a predominant lepidic growth pattern, or invasive mucinous adenocarcinoma.Lee et al. correlated this sign with nodular lesions in pulmonary adenocarcinoma with a lepidic growth pattern.

The cheerios sign may also be associated with other conditions, such as Langerhans cell histiocytosis or meningothelial pulmonary nodules (Chou et al., 2013). It is critical to distinguish nodules exhibiting the cheerios sign from cavitated nodules, where the central cavity results from necrosis rather than tissue proliferation around an airway.

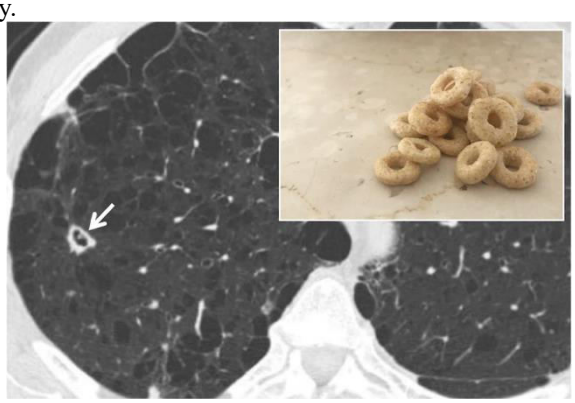

fig. 5

Crazy Paving

The "crazy paving" appearance is a nonspecific radiological sign characterized by increased pulmonary parenchymal density with a ground-glass appearance, overlaid by a reticular thickening of the interlobular and intralobular septa (Fig. 6) (Maimon & Heimer, 2010). This imaging feature was initially observed in cases of pulmonary alveolar proteinosis, a rare condition involving alveolar filling with proteinaceous, lipid-rich material. This process is often accompanied by interstitial inflammation, which reproduces the secondary pulmonary lobule as polygonal shapes. Other potential causes include bacterial pneumonia, Pneumocystis jirovecii infection, drug-induced lung disease, and pulmonary adenocarcinoma with a lepidic growth pattern. Additionally, the crazy paving pattern may be associated with interstitial lung diseases, such as nonspecific

interstitial pneumonia (NSIP), cryptogenic organizing pneumonia (COP), sarcoidosis, and pulmonary hemorrhage resulting from conditions like granulomatosis with polyangiitis and Goodpasture's syndrome.

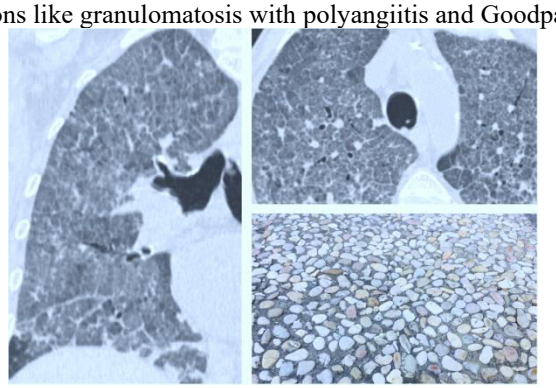

fig. 6

Comet Tail Sign

The "comet tail" sign is a curvilinear opacity extending from a subpleural mass toward the ipsilateral hilum (Fig. 7). First described by Verschakelen this sign reflects distorted bronchovascular structures contiguous to a round atelectasis. This phenomenon is frequently associated with thickened adjacent pleura and displacement of nearby fissures. Round atelectasis represents a rare form of parenchymal collapse occurring near the pleural surface, often exhibiting an air bronchogram within its structure. Historically referred to as "Blesovsky syndrome" or "atelectatic pseudotumor," this presentation can mimic a neoplastic lesion. Round atelectasis is often attributed to irritant substances on the pleural surface, such as asbestos, which leads to pleural thickening and contraction of the adjacent pulmonary parenchyma into a rounded form.

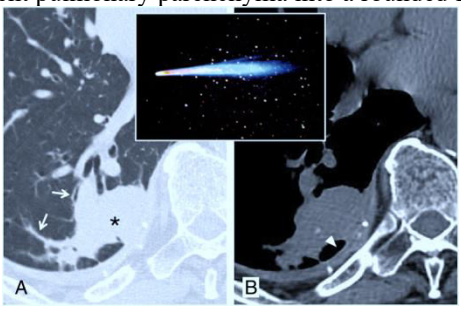

fig. 7

Dark Bronchus Sign

The "dark bronchus sign" is characterized by the visualization of an apparently darker bronchus within a region of lung parenchyma exhibiting a ground-glass appearance (Fig. 8). This sign differs from the "air bronchogram," where bronchial structures are seen traversing an area of pulmonary consolidation. Yadav et al. described this sign in a case involving a 50-year-old HIV-infected patient with Pneumocystis jirovecii pneumonia. The darker appearance of the bronchus on MDCT imaging was attributed to increased density in the adjacent lung parenchyma. Pneumocystis infection typically presents with patchy or diffuse ground-glass opacities, centrilobular nodules, pleural effusions, and lymphadenopathy. In some instances, the increase in lung density is subtle and diffuse, making it challenging to discern without healthy parenchyma for comparison. Under such circumstances, the dark bronchus sign serves as a critical diagnostic clue for identifying Pneumocystis jirovecii infection (Yadav et al., 2007).

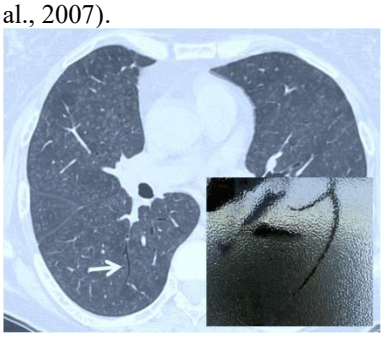

fig. 8

Doughnut Sign

The "doughnut sign" is observed in the lateral chest radiograph or the lateral scout image of a CT scan. It appears as a complete radiopaque ring resembling a doughnut (Fig. 9). This appearance is formed by the normal contours of the right and left pulmonary arteries and the aortic arch on the anterior and superior aspects,

with mediastinal lymphadenopathy in the inferior portion. The lymph nodes completing the radiopaque ring are located in subcarinal, hilar, and retrocarinal regions. The radiolucent center of the doughnut corresponds to the trachea and bronchi of the upper lobes. This sign is frequently associated with conditions such as tuberculosis and lymphoma (Mahomed et al., 2011).

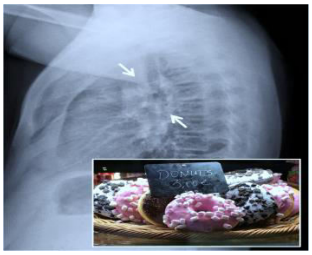

fig. 9

Eggshell Calcifications

The "eggshell" calcifications are radiological findings visible on chest radiographs and CT scans. They are characterized by lymph nodes with lamellar calcifications (Fig. 10) and are associated with various pathological conditions. The first documentation of these calcifications in the literature dates back to the late 1960s by Jacobson and Felson. According to criteria established by Jacobson "eggshell" calcifications are defined by the following features:

1. Calcifications located peripherally, with a minimum thickness of 2 mm, visible in at least two lymph nodes.
2. Calcifications that may be either intact or disrupted.
3. At least one lymph node exhibiting a diameter greater than 1 cm.
4. At least one lymph node displaying a complete calcified ring.
5. Lymph nodes demonstrating peripheral calcifications, occasionally extending to the central region.

These calcifications are nonspecific and may be identified in numerous diseases, including advanced sarcoidosis, silicosis, pneumoconiosis, scleroderma, amyloidosis, lymphoma post-radiotherapy, blastomycosis, and histoplasmosis.

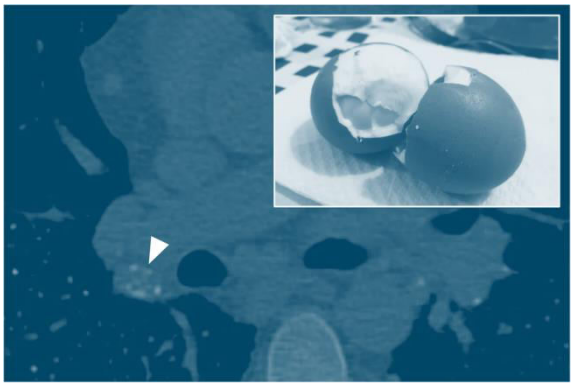

fig. 10

Feeding Vessel Sign

The "feeding vessel sign" is characterized by a pulmonary vascular branch extending toward a focal lesion and terminating within its structure (Fig. 11). This radiological sign has two primary implications: (1) the lesion may have a vascular origin, as seen in arterio-venous malformations or embolisms, and (2) it may suggest a neoplastic lesion, often associated with high neoangiogenic activity. Also referred to as the "fruits on the branch sign," it has been linked to metastases and septic emboli. This sign is also commonly observed in pulmonary infarcts or arterio-venous fistulas.

In 1992, Murata et al. conducted a pathological correlation study on this sign, demonstrating that in cases of neoplastic nodular lesions, particularly metastatic ones, the "feeding vessel sign" is attributable to an arterial vessel penetrating the lesion in only 18% of cases identified on CT scans. In contrast, 58% of cases showed displacement of the vessel, which proceeded adjacent to the nodule. Yudin reported in 2014 that the feeding vessel sign is rarely detected in lung tumors or granulomas (Yudin, 2023).

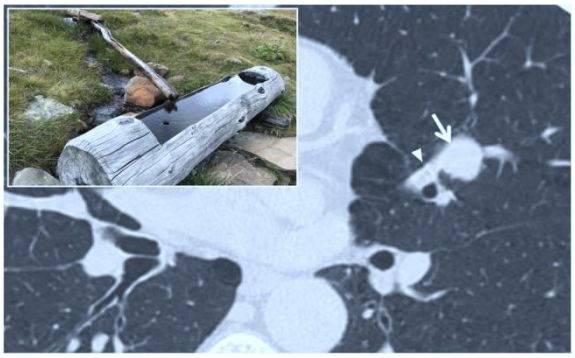

fig. 11

Finger-in-Glove Sign

The "finger-in-glove" sign is observed on chest radiographs and CT images, appearing as pulmonary opacities with characteristic shapes (linear, V-shaped, or Y-shaped) and well-defined, lobulated margins (Fig. 12). This sign is caused by dilated bronchial structures filled with mucoid material (bronchocele). The term was first introduced in 2003 by Nguyen, who described linear or branched opacities extending from the hilum to the lung periphery on posterior-anterior chest radiographs.

The "finger-in-glove" sign is commonly associated with two conditions:

1. **Inflammatory diseases**—such as cystic fibrosis, allergic bronchopulmonary aspergillosis, and asthma.
2. **Obstructive diseases**—both congenital (e.g., bronchial malformations) and acquired (e.g., foreign body obstruction).

fig. 12

Fleischner Sign

The "Fleischner sign" is defined as a prominent central pulmonary artery observed upstream of an obstruction (Fig. 13). It is typically caused by a large embolus in the central pulmonary artery or may also be associated with pulmonary hypertension. The sign was described by Felix George Fleischner and is a critical radiological indicator of pulmonary embolism on chest radiographs.

This sign is frequently observed in conjunction with the "knuckle sign," which refers to the abrupt cutoff of a pulmonary artery branch due to the presence of a blood clot, resembling the knuckle of a fist (Fig. 14). While the Fleischner sign is more apparent on chest radiographs, the knuckle sign is better visualized on CT images. Both are considered hallmark signs of pulmonary embolism (Kumaresh et al., 2015).

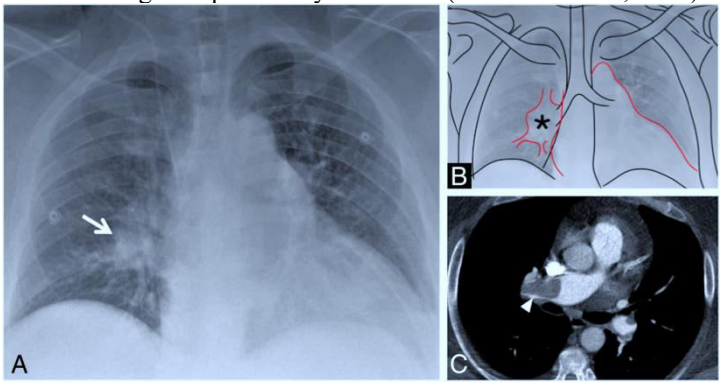

Fig. 13

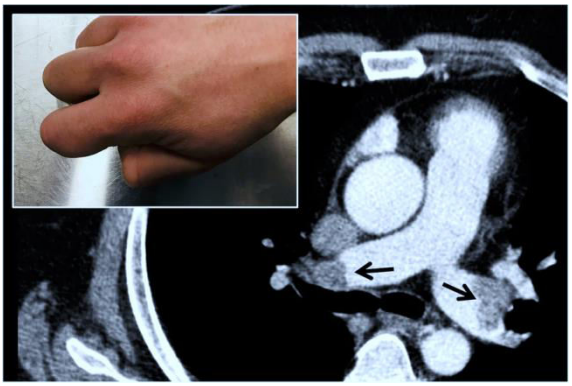

fig. 14

Galaxy Sign

The "galaxy sign" is a classic radiological finding of sarcoidosis observed on MDCT scans. It consists of a central lesion, typically larger than 1 cm, surrounded by satellite nodules (Fig. 15). In some cases, regions of ground-glass opacity may also be evident. This sign was first described in the literature by Nakatsu et al. who correlated it with pathological findings. The authors explained that these "sarcoid masses" are composed of multiple confluent granulomas, which are more distinctly visualized at the periphery of the lesions. Nakatsu et al. also described rare occurrences of cavitation within these masses in their series of cases.

The "galaxy sign" can also be associated with infectious diseases, where large nodules form due to the confluence of smaller nodules. This has been documented in cases of active tuberculosis, particularly when accompanied by tree-in-bud lesions (Heo et al., 2005).

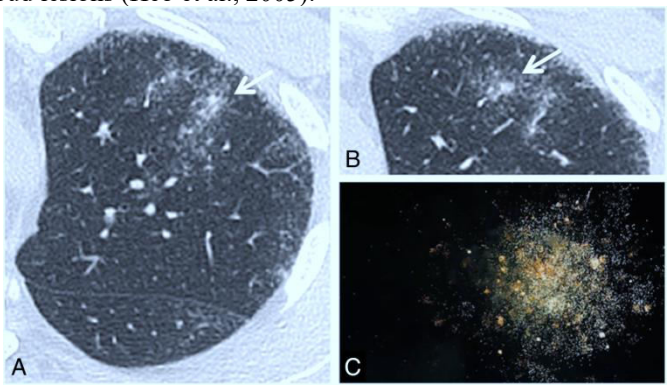

fig. 15

Ginkgo Leaf Sign

The "ginkgo leaf sign" is identified on anterior-posterior chest radiographs and is attributed to significant amounts of air in the subcutaneous tissues of the chest wall (Fig. 16). The gas outlines the fibers of the pectoralis major muscle, producing a pattern resembling the vein structure of a ginkgo leaf. This sign has been described in the literature as a typical imaging finding in patients with thoracic polytrauma (Ho & Gutierrez, 2009).

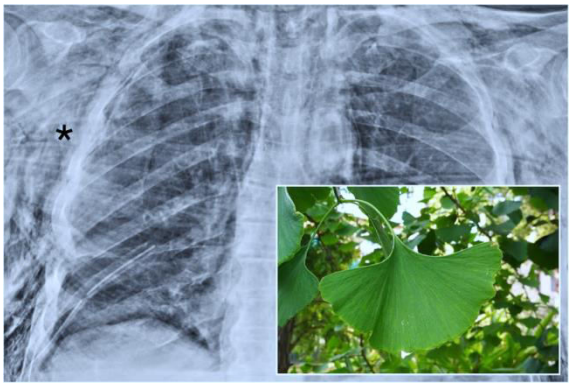

fig. 16

Golden S-Sign

The "Golden S-sign" refers to an "S"-shaped contour observed on posterior-anterior chest radiographs, indicative of right upper lobe atelectasis with an associated mass at the right hilum. It is also referred to as the

"reverse S sign of Golden" and was first described by Ross and Golden who linked it to right upper lobe collapse caused by bronchogenic carcinoma in the right hilum.
On radiographs, the superior and lateral segments of the "S" (concave inferiorly) correspond to the collapsed upper lobe, while the inferior and medial segments (convex inferiorly) represent the associated pulmonary mass. This sign is more distinctly visualized on MDCT scans (Fig. 17) and can also be observed in cases of lymphadenopathy or mediastinal tumors, in addition to bronchogenic carcinoma (Bunkar et al., 2014).

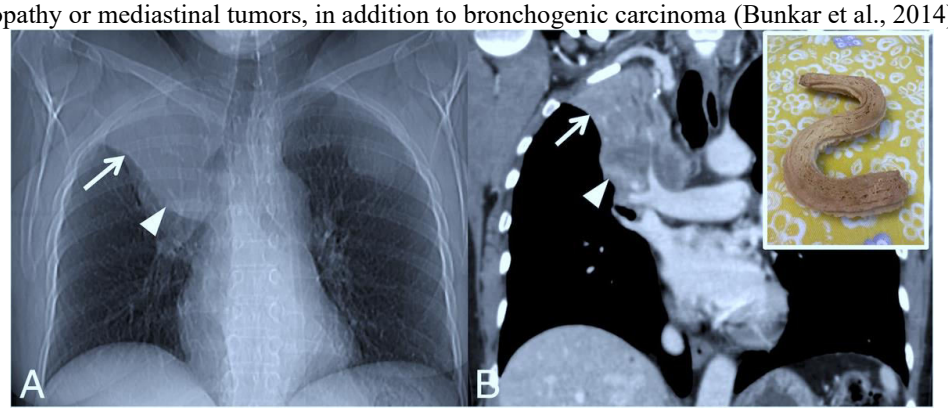

fig 17

Halo Sign

The "halo sign" appears on MDCT as a solid lesion surrounded by a peripheral ground-glass halo (Fig. 18). The ground-glass attenuation is typically indicative of a perilesional hemorrhagic process. This sign was first described by Kuhlman et al. as characteristic of angio-invasive aspergillosis. Over time, this radiological finding has been associated with various conditions, including neoplastic and non-neoplastic diseases (e.g., vasculitis, organizing pneumonia, pulmonary endometriosis).

The halo sign is often more pronounced in infectious diseases (Alves et al., 2016, p. 85), and the clinical context is crucial for differential diagnosis. In immunocompromised patients, the sign has been linked to fungal infections such as invasive aspergillosis, pulmonary candidiasis, and coccidioidomycosis, as well as lymphoproliferative disorders. In immunocompetent individuals, conditions presenting with the halo sign include primary neoplasms, metastases, vasculitis (e.g., Wegener's granulomatosis), sarcoidosis, and organizing pneumonia.

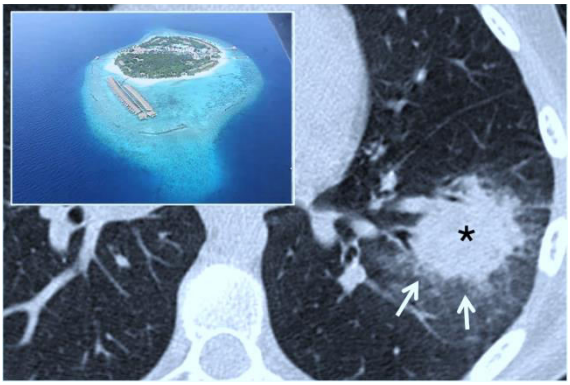

fig. 18

Headcheese Sign

The "headcheese sign" was introduced to radiological literature by Patel et al. in 2000 as a characteristic imaging feature of hypersensitivity pneumonitis. This pattern, visible on CT, is produced by the coexistence of ground-glass opacities, areas of air trapping, and normal lung regions (Fig. 19). It is most commonly observed on expiratory CT scans.

The sign arises when obstructive small-airway disease coincides with alveolar inflammatory infiltration. Although considered pathognomonic for chronic hypersensitivity pneumonitis (CHP), it may also occur in other conditions, such as infections with bronchiolitis or atypical cases of sarcoidosis involving alveoli. The term "headcheese sign" refers to the CT appearance of the pulmonary parenchyma, where lobular areas of differing densities resemble the European meat dish of the same name(Chong et al., 2014).

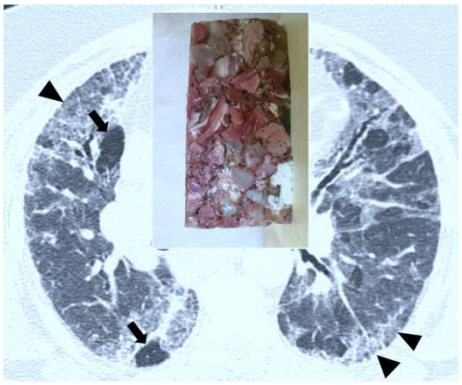

fig. 19

Honeycombing

The term "honeycomb appearance of the lung" was first used in Germany during the mid-19th century to describe bronchial malformations or cystic bronchiectasis. Later, other authors applied it to the typical appearance of usual interstitial pneumonia (UIP), which was described as "bronchial emphysema" or "cystic pulmonary cirrhosis." The modern definition of "honeycomb lung" originates from Oswald and Parkinson.

According to the Fleischner Society glossary, honeycombing is characterized by cystic spaces with defined walls located in subpleural regions, typically measuring 3–10 mm in diameter (Fig. 20). It represents the end-stage of parenchymal fibrosis, resulting in complete architectural distortion of the lung. Honeycombing predominantly affects the basal and peripheral lung regions. Extensive honeycombing is highly indicative of UIP, though it can also be found in other fibrotic conditions, such as chronic hypersensitivity pneumonia, stage IV sarcoidosis, and certain pneumonias. However, these cases typically show less extensive cystic degeneration with atypical distributions, such as mid-apical parenchymal involvement.

Recent guidelines from the Fleischner Society have modified the diagnostic criteria, allowing for the presence of a few subpleural cysts in a single layer to be defined as honeycombing if the pathological context is appropriate (Lynch et al., 2018).

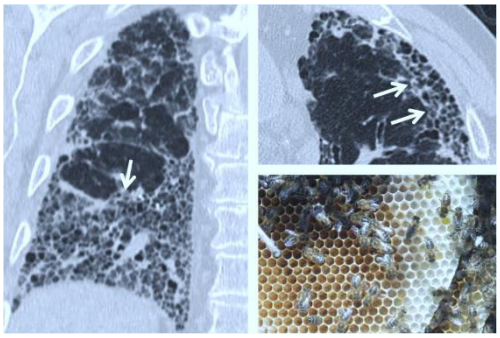

fig. 20

Interface Sign

The "interface sign" is a CT feature of fibrosing interstitial lung diseases. Normally, the boundary between subpleural or mediastinal fat and pulmonary parenchyma appears linear and smooth. However, in the presence of interstitial fibrosis, thickening and focal retractions of the lung parenchyma create irregularities in the interface between the lung parenchyma, vessels, bronchi, and visceral pleura.

This produces a "jagged" appearance (Fig. 21) and is observed in all fibrosing lung diseases, including UIP, nonspecific interstitial pneumonia (NSIP), and CHP. It is regarded as a significant imaging finding for identifying these pathological conditions (Sverzellati et al., 2015).

fig. 21

Monod Sign

The "Monod sign," first described by Pesle and Monod refers to the presence of air surrounding a mycetoma, often an aspergilloma, within a pre-existing cavity (Fig. 22). This sign holds a different prognostic significance compared to the air crescent sign. Typically observed in immunocompetent individuals with a history of prior cavitating or cystic lung conditions, such as tuberculosis, it is frequently associated with symptoms like hemoptysis. In cases of aspergilloma, the fungal mass—composed of fungal hyphae, mucus, and cellular debris—within the cavity is mobile and shifts with changes in the patient's position. This mobility helps distinguish between a mass inside a cavity (Monod sign) and a cavitated mass (Nitschke et al., 2013).

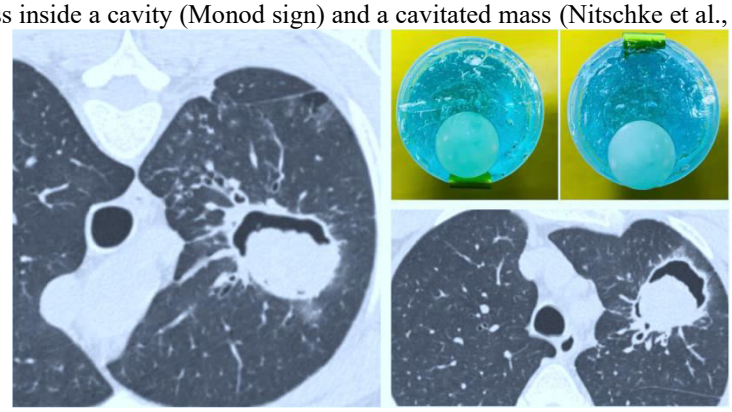

fig. 22

Mosaic Attenuation

The "mosaic attenuation" pattern, as visualized on CT imaging, describes alternating regions of differing attenuation within the lung parenchyma (Fig. 23). Eber et al. first introduced this term as indicative of bronchiolitis and King et al. further elaborated its association with chronic pulmonary embolism in 1994. It is essential to consider that minor degrees of parenchymal inhomogeneity may be physiological, such as increased attenuation in dependent lung regions or central pulmonary areas due to greater perfusion. The mosaic pattern, however, is a nonspecific radiological sign and can be observed in various pathological contexts, including small airway obstruction, vascular occlusion, and parenchymal disease. Specific CT features can help differentiate these conditions. For instance, in hypoattenuated regions with smaller vessels, the cause might be vascular, such as chronic pulmonary embolism. If expiratory CT scans reveal no density changes in hypoattenuated areas, this indicates air trapping due to small airway disease, such as bronchiolitis. In contrast, if infiltrative processes in the pulmonary interstitium are present, affected areas show increased attenuation, with no difference in vascular caliber between pathological and healthy regions. Such mosaic patterns can occur in conditions like Pneumocystis jirovecii pneumonia (Ridge et al., 2011).

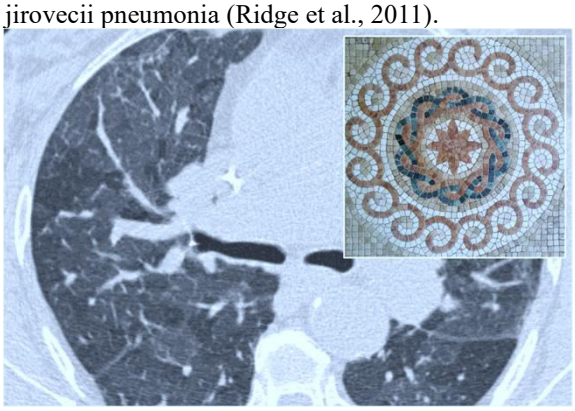

fig. 23

Oreo Cookie Sign

The "Oreo cookie sign," recently described in the title of a research paper, represents the radiological appearance of pericardial effusion seen on lateral chest radiographs (Fig. 24). In this context, increased pericardial radiopacity is anteriorly and posteriorly bordered by two radiolucent lines, corresponding to pericardial fat and epicardial fat, respectively (Li et al., 2017). This sign is more frequently and distinctly observed on CT images.

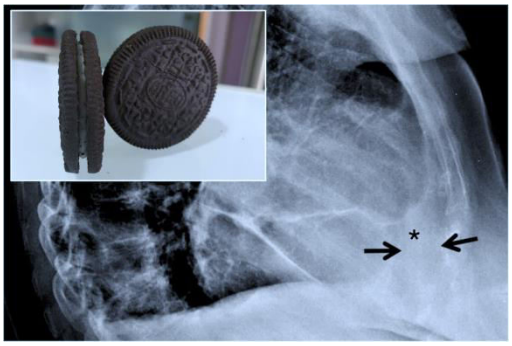

fig. 24

Polo Mint Sign

In thoracic imaging, the "polo mint sign" is associated with acute pulmonary embolism, characterized by the appearance of a thrombosed vessel on axial CT planes (Fig. 25). Wittram et al. first reported this sign in a 2004 study on imaging features of acute pulmonary embolism. It arises in contrast-enhanced CT scans when contrast material surrounds a central filling defect within a vessel, paralleling the "railway track sign," which occurs when the vessel is viewed longitudinally.

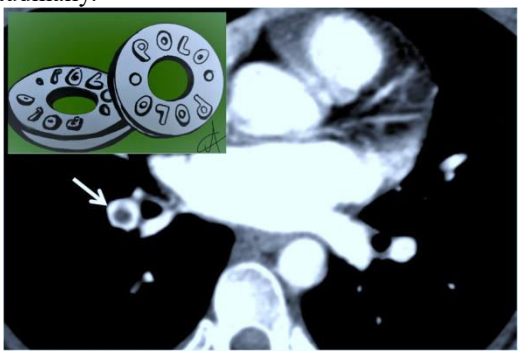

fig. 25

Popcorn Calcification

The term "popcorn calcification" refers to amorphous, ring-shaped calcifications that resemble popcorn (Fig. 26). Within the lung, such calcifications, found in well-defined nodules, are strongly indicative of benign lesions, particularly hamartomas. Briccoli et al. reported that only 10% of pulmonary hamartomas exhibit popcorn calcifications. These calcifications are better visualized on CT scans, which also reveal intralesional fat in approximately 60% of cases. While benign lesions often display widespread, centralized, or stratified calcifications, malignant lesions are more commonly associated with punctate or eccentric calcifications, as seen in carcinoid tumors or metastatic osteosarcomas (Khan et al., 2010).

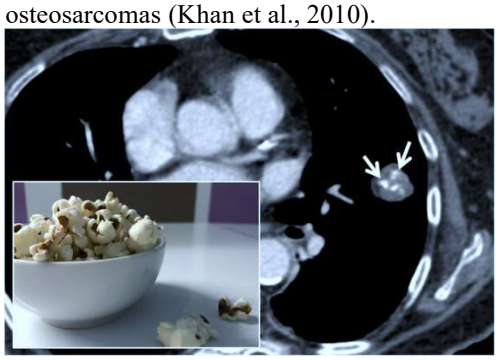

fig. 26

Positive Bronchus Sign

On chest CT imaging, the "positive bronchus sign" is defined by an air-filled bronchus—visualized as a tubular hypoattenuating structure—extending toward a peripheral nodule (Fig. 27). Naidich et al. initially emphasized its importance in 1988 as a predictive indicator for diagnostic bronchoscopy. Singh provided a comprehensive explanation of this sign. The air-filled bronchus may extend into the nodule, forming an air bronchogram. This sign is most associated with larger masses (≥ 3 cm) or lesions with spiculated margins and is frequently observed in malignant conditions, such as pulmonary adenocarcinomas with a lepidic pattern. Tsuboi et al. identified four bronchus-mass relationship types: (1) the bronchus terminates at the nodule; (2) the bronchus continues into the nodule; (3) the bronchus is compressed but retains an intact mucosa; and (4) the bronchus shows submucosal tumor spread, resulting in irregular thinning. These relationships inform biopsy strategies,

with types (1) and (2) favoring biopsy, while types (3) and (4) are better suited to transbronchial aspiration (Ernst &Anantham, 2010).

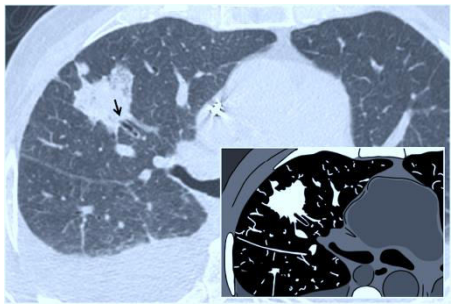

fig. 27

Railway Track Sign

The "railway track sign" is a CT finding in acute pulmonary embolism cases. It occurs when a pulmonary artery viewed longitudinally reveals a central filling defect—caused by a thrombus—flanked by peripheral contrast enhancement, creating a rail track-like appearance (Fig. 28). This sign corresponds to the previously described "polo mint sign," where the vessel is visualized in cross-section. In chronic pulmonary embolism, this sign is absent due to the eccentric positioning of the thrombus within the vessel.

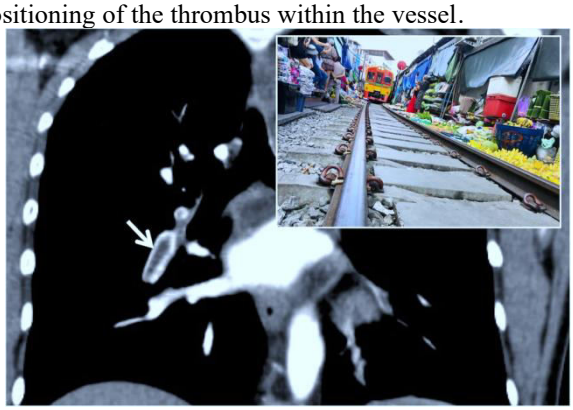

fig. 28

Scimitar Sign

Scimitar syndrome is an uncommon cardiopulmonary anomaly characterized by a left-to-right acyanotic shunt caused by anomalous pulmonary venous return. Initially described it is most often observed in the right hemithorax and is associated with pulmonary hypoplasia. The anomalous venous drainage typically occurs into (a) the inferior vena cava (most commonly), (b) the right atrium, or (c) a branch of the portal venous system. In approximately one-third of cases, the scimitar sign (Fig. 29) can be identified on chest radiographs of affected individuals, where the aberrant vessel appears as a radiopaque tubular structure parallel to the right cardiac border, resembling the curved blade of a Turkish scimitar. Additional imaging findings include ipsilateral mediastinal shift and lung hypoplasia. Both CT angiography and MR angiography are highly effective in delineating this vascular anomaly and differentiating it from other conditions such as pulmonary sequestration and pulmonary vein varices, which are the primary differential diagnoses (Nazarian et al., 2013).

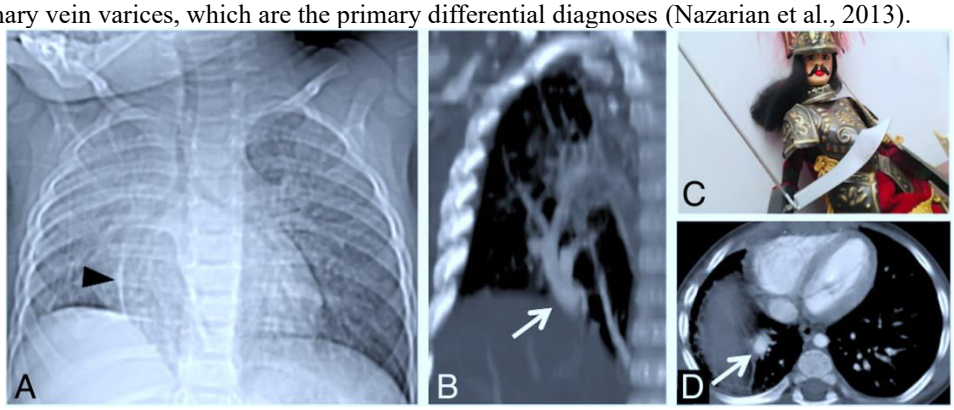

fig. 29

Signet Ring Sign

The “signet ring sign” is a radiological feature observable on thoracic CT scans, described in the literature by Hugue Ouellette. This sign involves an ectatic bronchus with thickened walls, which, when seen in cross-section alongside the corresponding pulmonary artery, resembles a signet ring (Fig. 30). Normally, the sizes of the

bronchus and artery are comparable, but this ratio is disrupted in cases of bronchiectasis, with the bronchus being enlarged.

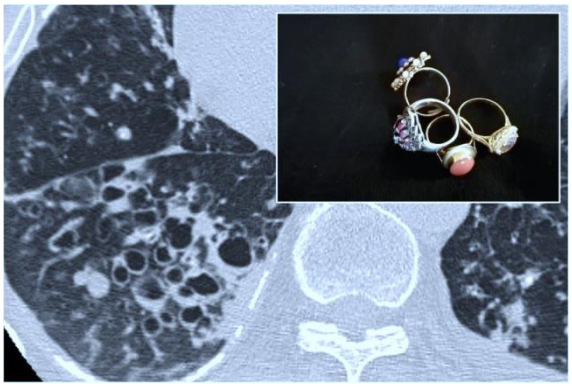

fig. 30

Snowstorm Sign

The "snowstorm sign" or "snowstorm appearance" is caused by the miliary spread of numerous micronodules (1–2 mm) throughout the pulmonary parenchyma (Fig. 31) and is visible on chest radiographs. Yudin et al. initially described this appearance in the context of metastatic nodules from vascular tumors such as thyroid carcinoma and renal cell carcinoma, distinguishing it from "cannonball metastases," which are larger, well-defined nodules often originating from gastrointestinal malignancies (Yudin, 2014). The snowstorm appearance has also been documented in cases of miliary distribution of metastatic nodules from papillary thyroid carcinoma. More frequently, confirmation of the diagnosis requires MDCT imaging to identify nodules of truly miliary size. Differential diagnoses include miliary tuberculosis, fungal infections (e.g., histoplasmosis, coccidioidomycosis), sarcoidosis, and calcifications secondary to chickenpox infection.

A pulmonary snowstorm appearance has also been reported by Bhalotra et al. in a 28-year-old male patient with diffuse lung micronodules caused by pulmonary alveolar microlithiasis.

The use of MDCT imaging to assess nodule margins is essential for differential diagnosis: poorly defined margins are more likely associated with distal airspace involvement, while well-defined nodules typically suggest interstitial pathology. Clinical history, additional radiological findings, and comorbid conditions can further aid in diagnosis. For instance, these fine parenchymal micronodules may suggest a neoplastic origin in the presence of a known primary tumor or sarcoidosis in cases with enlarged mediastinal lymph nodes.

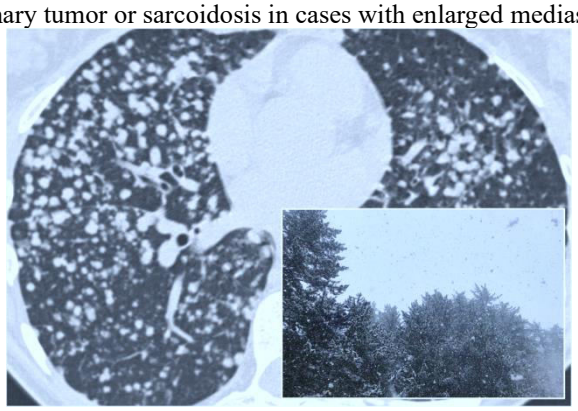

fig. 31

Sunburst Sign

The "sunburst sign" refers to a pulmonary nodule or mass with spiculated, irregular margins resembling sunrays, a finding described by O'Donovan. These spiculations are formed by distorted blood vessels or thickened septa radiating outward from the nodule (Fig. 32). This sign is highly suggestive of malignancy, particularly pulmonary adenocarcinoma. The presence of spiculated margins is considered a significant risk factor for malignancy, with odds ratios ranging from 2.2 to 2.5 in screening studies of pulmonary nodules (Choromańska & Macura, 2012). In the differential diagnosis, the "galaxy sign," which refers to benign micronodules surrounding a nodule in sarcoidosis, should also be considered.

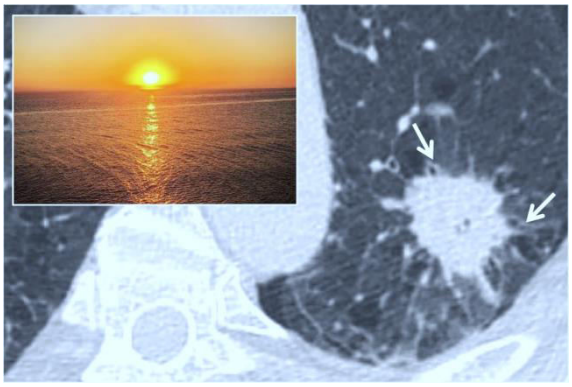

fig. 32

Tree-in-Bud Pattern

The “tree-in-bud” pattern, first described by Im et al., is a radiological feature characterized by centrilobular nodularities with linear branching, resembling a flowering tree (Fig. 33). This pattern is caused by dilation and filling of terminal bronchioles with mucus, pus, or other materials and can be found in a wide range of lung diseases. These include distal airway diseases, bacterial, viral, and fungal infections, congenital conditions (e.g., cystic fibrosis), idiopathic diseases (e.g., bronchiolitis obliterans), inhalation or aspiration syndromes, immune disorders, connective tissue diseases, and tumors causing embolization of centrilobular arterioles.

Tree-in-bud opacities are often accompanied by additional parenchymal changes, such as bronchial wall thickening, consolidations, or areas of ground-glass opacity. In some cases, these opacities coexist with bronchiectasis and may mimic small airway obstruction, creating a mosaic attenuation pattern on imaging.

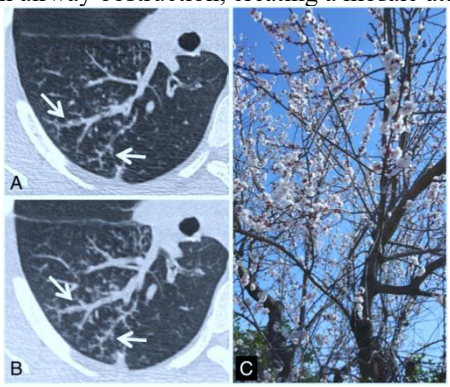

fig. 33

Tram Track Sign

The tram track sign, seen in patients with cylindrical bronchiectasis, is depicted as parallel line opacities on chest radiographs that resemble tram tracks (Fig. 34). This appearance, caused by thickened bronchial walls, is more accurately visualized on CT scans, where the pathological bronchus can be clearly delineated along its major axis. This sign is commonly observed in individuals with pulmonary involvement in cystic fibrosis and in patients with chronic obstructive pulmonary disease (COPD) with severe bronchiectasis.

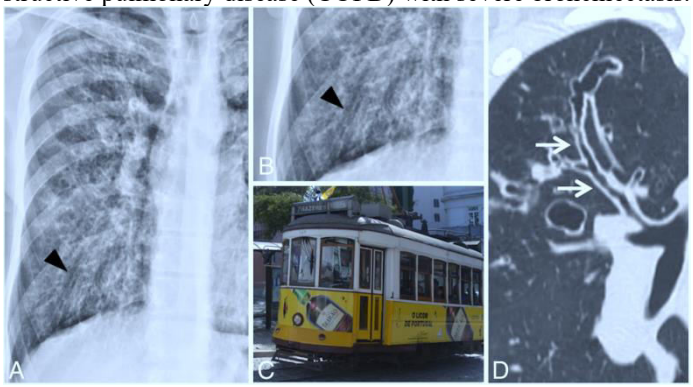

fig. 34

Miscellaneous Radiological Signs

Various other thoracic conditions and abnormalities produce radiological signs resembling symbols, natural objects, or geometric shapes. For instance, pulmonary hydatid disease is characterized by the “serpent sign” and the “water lily sign.” The “water lily sign” results from detachment of the endocyst membrane from the pericyst,

causing the membrane to collapse and float within the hydatid fluid, mimicking a water lily(Kaya & Kerimoğlu, 2017). The "serpent sign" is indicative of an internal rupture of the hydatid cyst, with collapsed parasitic membranes visible within the cyst.

The "cervicothoracic sign" and "hilum overlay sign" are useful for localizing masses in the superior mediastinum or hilum, respectively, based on the silhouette principle. The "deep sulcus sign" indicates pneumothorax on a supine chest radiograph, with radiolucency at the cardiophrenic or costophrenic angles. The "Hampton's hump" appears as a small peripheral triangular consolidation due to lung atelectasis in pulmonary embolism.

Finally, the "Swiss cheese sign" describes the appearance of lung parenchyma with pneumatocele formations, resembling holes in Swiss cheese, often following trauma, mechanical ventilation, or infections.

Conclusion

Chest CT imaging provides unparalleled insights into the diagnosis and understanding of pulmonary diseases, where radiological signs play an indispensable role. These signs, often derived from metaphorical associations with natural or symbolic images, bridge complex diagnostic processes and enhance memorability for clinicians. By correlating specific imaging patterns with underlying pathological processes, such signs enable more precise diagnoses and informed clinical decision-making.

From pathognomonic indicators such as the air bronchogram and honeycombing, to nonspecific patterns like mosaic attenuation and crazy paving, the detailed recognition and interpretation of these signs empower radiologists and pulmonologists in navigating diverse differential diagnoses. Modern imaging techniques, including multidetector CT and CT angiography, further augment the visualization and understanding of complex thoracic abnormalities, expanding the diagnostic toolkit available to healthcare providers.

This review not only reinforces the diagnostic importance of well-documented radiological signs but also emphasizes their evolving relevance in light of emerging imaging modalities. The enduring value of these metaphorical signs lies in their ability to simplify intricate imaging findings, making them accessible and actionable within clinical practice. Ultimately, a nuanced understanding of radiological signs strengthens diagnostic accuracy and contributes to improved patient outcomes in the realm of pulmonary medicine.

References

Algın, O., Gökalp, G., & Topal, U. (2011). Signs in chest imaging. *Diagnostic and Interventional Radiology (Ankara, Turkey)*, *17*(1), 18–29. https://doi.org/10.4261/1305-3825.DIR.2901-09.1

Alves, G. R. T., Marchiori, E., Irion, K., Nin, C. S., Watte, G., Pasqualotto, A. C., Severo, L. C., & Hochhegger, B. (2016). The halo sign: HRCT findings in 85 patients. *Jornal Brasileiro de Pneumologia*, *42*, 435–439. https://doi.org/10.1590/S1806-37562015000000029

Bunkar, M. L., Takhar, R., Arya, S., & Biswas, R. (2014). Golden 'S' sign. *Case Reports*, *2014*, bcr2014207844. https://doi.org/10.1136/bcr-2014-207844

Chong, B. J., Kanne, J. P., & Chung, J. H. (2014). Headcheese sign. *Journal of Thoracic Imaging*, *29*(1), W13. https://doi.org/10.1097/RTI.0000000000000067

Choromańska, A., & Macura, K. J. (2012). Evaluation of solitary pulmonary nodule detected during computed tomography examination. *Polish Journal of Radiology*, *77*(2), 22–34.

Chou, S.-H. S., Kicska, G., Kanne, J. P., & Pipavath, S. (2013). Cheerio Sign. *Journal of Thoracic Imaging*, *28*(1), W4. https://doi.org/10.1097/RTI.0b013e31827944d2

Ernst, A., & Anantham, D. (2010). Bronchus sign on CT scan rediscovered. *Chest*, *138*(6), 1290–1292. https://doi.org/10.1378/chest.10-0892

Godoy, M. C. B., Viswanathan, C., Marchiori, E., Truong, M. T., Benveniste, M. F., Rossi, S., & Marom, E. M. (2012). The reversed halo sign: Update and differential diagnosis. *British Journal of Radiology*, *85*(1017), 1226–1235. https://doi.org/10.1259/bjr/54532316

Hansell, D. M., Bankier, A. A., MacMahon, H., McLoud, T. C., Müller, N. L., & Remy, J. (2008). Fleischner Society: Glossary of terms for thoracic imaging. *Radiology*, *246*(3), 697–722. https://doi.org/10.1148/radiol.2462070712

Heo, J.-N., Choi, Y. W., Jeon, S. C., & Park, C. K. (2005). Pulmonary tuberculosis: Another disease showing clusters of small nodules. *AJR. American Journal of Roentgenology*, *184*(2), 639–642. https://doi.org/10.2214/ajr.184.2.01840639

Ho, M.-L., & Gutierrez, F. R. (2009). Chest radiography in thoracic polytrauma. *AJR. American Journal of Roentgenology*, *192*(3), 599–612. https://doi.org/10.2214/AJR.07.3324

Kaya, H. E., & Kerimoğlu, Ü. (2017). The water lily sign. *Abdominal Radiology*, *42*(11), 2772–2773. https://doi.org/10.1007/s00261-017-1183-7

Khan, A. N., Al-Jahdali, H., AL-Ghanem, S., & Gouda, A. (2009). Reading chest radiographs in the critically ill (Part II): Radiography of lung pathologies common in the ICU patient. *Annals of Thoracic Medicine*, *4*(3), 149. https://doi.org/10.4103/1817-1737.53349

Khan, A. N., Al-Jahdali, H. H., Allen, C. M., Irion, K. L., Al Ghanem, S., & Koteyar, S. S. (2010). The calcified lung nodule: What does it mean? *Annals of Thoracic Medicine*, *5*(2), 67–79. https://doi.org/10.4103/1817-1737.62469

Kumaresh, A., Kumar, M., Dev, B., Gorantla, R., Sai, P. V., & Thanasekaraan, V. (2015). Back to Basics—'Must Know' Classical Signs in Thoracic Radiology. *Journal of Clinical Imaging Science*, *5*, 43. https://doi.org/10.4103/2156-7514.161977

Legouge, C., Caillot, D., Chrétien, M.-L., Lafon, I., Ferrant, E., Audia, S., Pagès, P.-B., Roques, M., Estivalet, L., Martin, L., Maitre, T., Bastie, J.-N., & Dalle, F. (2014). The Reversed Halo Sign: Pathognomonic Pattern of Pulmonary Mucormycosis in Leukemic Patients With Neutropenia? *Clinical Infectious Diseases*, *58*(5), 672–678. https://doi.org/10.1093/cid/cit929

Li, I., Greenstein, J., & Hahn, B. (2017). Pericardial Effusion With Oreo Cookie Sign. *The Journal of Emergency Medicine*, *52*(5), 756–757. https://doi.org/10.1016/j.jemermed.2017.01.015

Lynch, D. A., Sverzellati, N., Travis, W. D., Brown, K. K., Colby, T. V., Galvin, J. R., Goldin, J. G., Hansell, D. M., Inoue, Y., Johkoh, T., Nicholson, A. G., Knight, S. L., Raoof, S., Richeldi, L., Ryerson, C. J., Ryu, J. H., & Wells, A. U. (2018). Diagnostic criteria for idiopathic pulmonary fibrosis: A Fleischner Society White Paper. *The Lancet Respiratory Medicine*, *6*(2), 138–153. https://doi.org/10.1016/S2213-2600(17)30433-2

Mahomed, N., Hleza, B., & Andronikou, S. (2011). The doughnut sign: Clinical images. *South African Journal of Child Health*, *5*(4), 126–127. https://doi.org/10.10520/EJC64829

Maimon, N., & Heimer, D. (2010). The crazy-paving pattern on computed tomography. *CMAJ*, *182*(14), 1545–1545. https://doi.org/10.1503/cmaj.091422

Marchiori, E., Zanetti, G., & Hochhegger, B. (2015). Reversed halo sign. *Jornal Brasileiro De Pneumologia: Publicacao Oficial Da Sociedade Brasileira De Pneumologia E Tisilogia*, *41*(6), 564. https://doi.org/10.1590/S1806-37562015000000235

Marchiori, E., Zanetti, G., Meirelles, G. S. P., Escuissato, D. L., Souza, A. S., & Hochhegger, B. (2011). The Reversed Halo Sign on High-Resolution CT in Infectious and Noninfectious Pulmonary Diseases. *American Journal of Roentgenology*, *197*(1), W69–W75. https://doi.org/10.2214/AJR.10.5762

Nazarian, J., Kanne, J. P., & Rajiah, P. (2013). Scimitar Sign. *Journal of Thoracic Imaging*, *28*(4), W61. https://doi.org/10.1097/RTI.0b013e318292043e

Nitschke, A., Sachs, P., Suby-Long, T., & Restauri, N. (2013). Monod sign. *Journal of Thoracic Imaging*, *28*(6), W120. https://doi.org/10.1097/RTI.0000000000000042

Ridge, C. A., Bankier, A. A., & Eisenberg, R. L. (2011). Mosaic attenuation. *AJR. American Journal of Roentgenology*, *197*(6), W970-977. https://doi.org/10.2214/AJR.11.7067

Sverzellati, N., Lynch, D. A., Hansell, D. M., Johkoh, T., King, T. E., & Travis, W. D. (2015). American Thoracic Society-European Respiratory Society Classification of the Idiopathic Interstitial Pneumonias: Advances in Knowledge since 2002. *Radiographics: A Review Publication of the Radiological Society of North America, Inc*, *35*(7), 1849–1871. https://doi.org/10.1148/rg.2015140334

Yadav, P., Seith, A., & Sood, R. (2007). The 'dark bronchus' sign: HRCT diagnosis of: Pneumocystis carinii: pneumonia. *Annals of Thoracic Medicine*, *2*(1), 26. https://doi.org/10.4103/1817-1737.30359

Yella, L. K., Krishnan, P., & Gillego, V. (2005). The air crescent sign: A clue to the etiology of chronic necrotizing pneumonia. *Chest*, *127*(1), 395–397. https://doi.org/10.1378/chest.127.1.395

Yudin, A. (2014). Snowstorm Sign and Cannonball Metastases. In A. Yudin (Ed.), *Metaphorical Signs in Computed Tomography of Chest and Abdomen* (pp. 27–27). Springer International Publishing. https://doi.org/10.1007/978-3-319-04013-4_14

Yudin, A. (2023). Feeding Vessel Sign or Fruits on the Branch Sign. In A. Yudin (Ed.), *Metaphorical Signs in Computed Tomography of Chest and Abdomen* (pp. 29–30). Springer International Publishing. https://doi.org/10.1007/978-3-031-24494-0_15